PLASMA-CATALYTIC SYSTEM WITH WIDE-APERTURE ROTATING GLIDING DISCHARGE

O.A. Nedybaliuk, I.I. Fedirchyk, V.Ya. Chernyak

Taras Shevchenko National University of Kyiv, Kyiv, Ukraine

E-mail: oanedybaliuk@gmail.com

This paper presents the results of the study of the wide-aperture rotating gliding discharge which was used for the plasma-catalytic reforming of hydrocarbons into synthesis gas. The photographs were compared with the oscillograms that represented the voltage of the wide-aperture rotating gliding discharge. The emission spectra of the plasma torch of the wide-aperture rotating gliding discharge were investigated for cases of when the reaction chamber was supplied with air and ethanol-air mixture. The distributions of electron T_e, vibrational T_v and rotational T_r temperatures alongside the plasma torch inside the reaction chamber were determined.

PACS: 50., 52., 52.50.Dg

INTRODUCTION

Sustainable development [1] demands the use of renewable raw materials and the minimization of waste generated during the production of materials required by humanity. Plasma-catalytic reforming [2] is one of the approaches to the reforming of renewable raw materials into synthesis gas that comply with the conditions of sustainability [1, 3]. Plasma-catalytic reforming systems have two main chambers: the discharge chamber, which provides oxidant activation, and the reaction chamber in which activated oxidant interacts with hydrocarbon. During the plasma-catalytic reforming, discharge chamber is supplied only with an oxidant, meanwhile, the reaction chamber is supplied with the mixture of oxidant and hydrocarbon. Discharge generates active species (radicals, ions, electrons, excited atoms and molecules), which initiate reforming. Therefore, the sources of non-equilibrium (non-thermal) plasma with the high service life of electrodes play a vital part in the realization of plasma-catalytic approach. Wide-aperture rotating gliding discharge [4] can be such a source.

1. EXPERIMENTAL SET-UP

Fig. 1 shows the simplified scheme of the plasma-catalytic system with wide-aperture rotating gliding discharge. The plasma-catalytic system with wide-aperture rotating gliding discharge consists of the discharge chamber (1) and quartz reaction chamber (2) (100 mm high and with 36 mm inner diameter). The discharge was ignited between the internal T-shaped stainless-steel anode (3) 25 mm in diameter and external grounded stainless-steel cathode (4), which had an aperture 20 mm in diameter in the middle. Rotating gliding discharge was powered by БП-100 power source (PS), which provided up to 7 kV output voltage and was paired with 33 kOhm ballast resistance (R_b).

Discharge voltage and current were measured by a voltmeter (V) and an ammeter (A). A digital oscilloscope (5) was used to obtain voltage and current oscillograms with the help of 1/480 voltage divider and 10 Ohm shunt resistor (R_1). Optical emission spectra of the plasma torch in the quartz reaction chamber were registered by using a system that included an optical fiber (6), Solar TII (S-150-2-3648 USB) spectral device (7), and a PC (8). Spectrometer operated in 200…1000 nm wavelength range. PC was used to control the measurements and to process data collected by the spectrometer.

Plasma of rotating gliding discharge when the system was supplied only by air and the torch in the reaction chamber during the plasma-catalytic reforming of ethanol were investigated using optical emission spectroscopy.

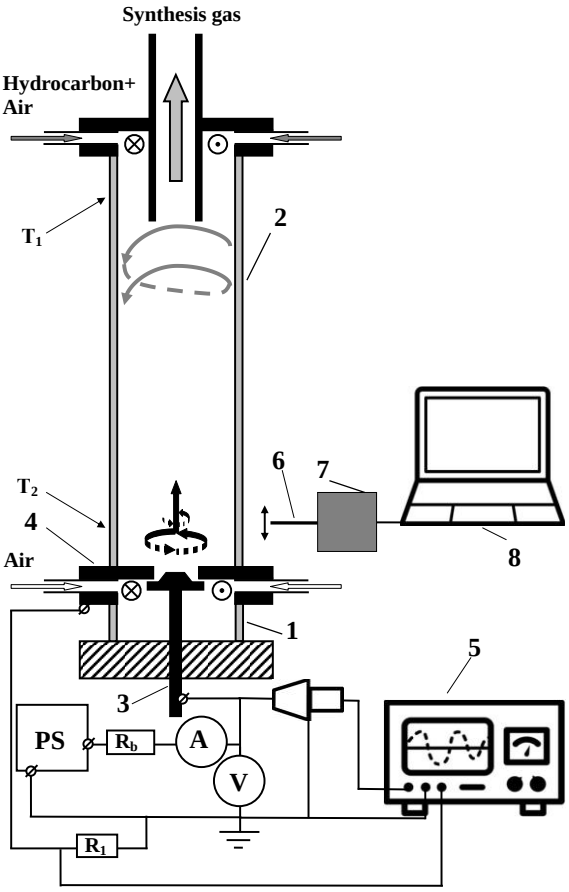

Fig. 1. Simplified scheme of the plasma-catalytic system with wide-aperture rotating gliding discharge: 1 – discharge chamber; 2 – quartz reaction chamber; 3 – T-shaped stainless-steel electrode (anode); 4 – external stainless-steel electrode (cathode); 5 – digital oscilloscope; 6 – optical fiber; 7 – spectrometer; 8 – PC

The relative intensities method was used to find the excitation temperatures of atoms based on the population of excited levels and their distribution alongside the length of the reaction chamber. Vibrational and rotational temperatures and their distribution alongside the length of reaction chamber were determined by matching measured optical emission spectra with spectra modeled in SpecAir software.

2. RESULTS AND DISCUSSION

Fig. 2 shows a typical photograph of the wide-aperture rotating gliding discharge, which was taken at 33 ms exposure. The air flow into the discharge chamber was $G_d = 20$ L·min^{-1} and the minimal distance between electrodes was 1 mm. Ammeter and voltmeter showed that discharge current was 80 mA and discharge voltage was 1.8 kV. Previous research of rotating gliding discharge established that the image represents a single discharge channel that rotates and glides along the electrodes [4].

Discharge channel rotates clockwise in the direction of the air flow. At 33 ms exposure, the photograph was able to capture only a part of the path that was covered by the gliding of discharge channel. The path of the discharge channel has several stand out sections (see Fig. 2). Section a-e corresponds to the movement of the discharge channel along the cathode and f-g section correspond to the movement of the discharge channel along the anode. Movement of one of the ends of discharge channel along the cathode on sections A-B (a), C-D (b), F-E (c), G-h (d), K-L (e) is accompanied by the increase of discharge channel length. The transitions between the cathode points B-C, D-E, F-G are accompanied with the small decrease discharge channel length, while H-K (see Fig. 2) transition shows a sharp drop of discharge channel length. After this, the length of the discharge channel continues to increase, and discharge continues to move along the cathode (section e) and anode (section g). The increase of discharge channel length at the constant potential difference would have led to the drop of the electric field and the end of discharge. Therefore, support of the continuous discharge operation during the increase of discharge channel length requires the increase of the potential difference in the discharge channel, which, in turn, requires the increase of discharge voltage.

Indeed, typical voltage oscillogram (Fig. 3,a) of wide-aperture rotating gliding discharge without the quartz reaction chamber taken during the same regime that the photograph (see Fig. 2) has sections with both slow increase and a sharp decrease of the discharge voltage. Sections with the small but sharp drops of voltage B-C, D-E, F-G (see Fig. 3,a) correspond to the transitions B-C, D-E, F-G (see Fig. 2) that indicate small decreases of discharge channel length. The section with a significant and sharp voltage drop H-K (see Fig. 3,a) corresponds to the sharp decrease of discharge channel length marked by H-K (see Fig. 2) transition. Thus, the minimum of discharge voltage on the oscillogram corresponds to the minimal length of the discharge channel and the maximum of discharge voltage on the oscillogram corresponds to the maximal length of the discharge channel.

It should be noted that time interval between the minimal and maximal discharge voltage on the oscillograms is approximately 40…50 ms (see Fig. 3,a), which explains why 33 ms exposure allowed to capture only part of the discharge channel path on the photograph (see Fig. 2). In addition, discharge voltage presented on the oscillograms does not drop to zero at the minimal discharge channel length.

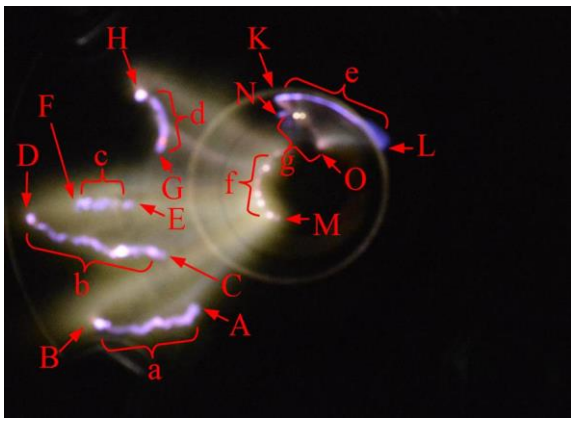

Fig. 2. Photo of wide-aperture rotating gliding discharge without quartz reaction chamber at exposure time 33 ms, G_d=20 L·min^{-1}

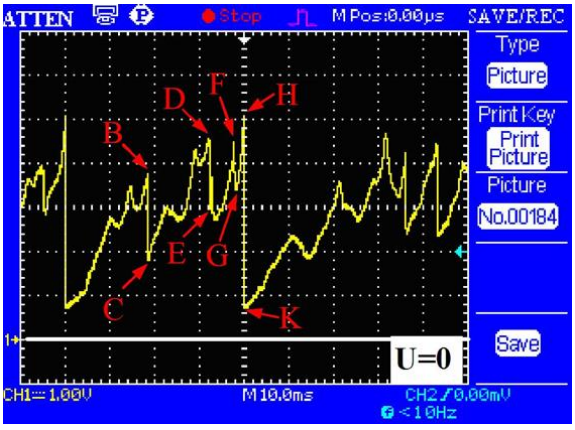

a

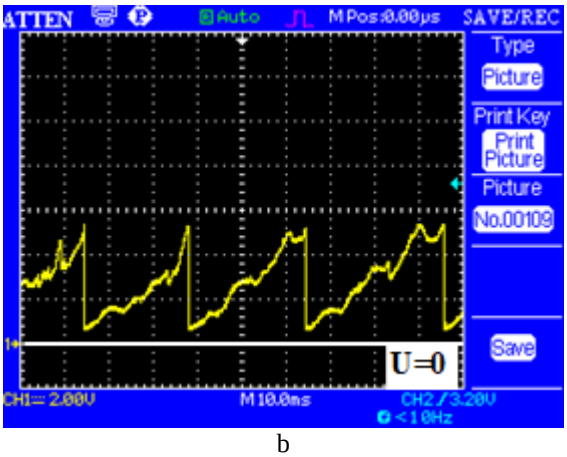

b

Fig. 3. Typical oscillograms of the voltage of wide-aperture rotating gliding discharge without (a) and with (b) quartz reaction chamber at G_d = 20 L·min^{-1} measured with the help of 1/480 voltage divider

The attachment of the quartz chamber had an impact on the voltage oscillograms. See Fig. 3,b shows typical voltage oscillogram of the wide-aperture rotating gliding discharge with the quartz reaction chamber at $G_d = 20$ L·min^{-1} air flow into the discharge chamber. The time interval between the minimal and maximal discharge voltage on the oscillograms (see Fig. 3,b) measured with the quartz reaction chamber is smaller (25…30 ms) than on oscillograms (see Fig. 3,a) measured without the reaction chamber (40…50 ms). This indicates that the time required for the discharge channel length to increase from its minimum to maximum decreased with the addition of quartz reaction chamber. At the same time, the average minimal and maximal values of discharge voltage didn't change. This behavior of rotating gliding discharge can be connected to the changes in gas dynamics.

Quartz chamber limited the surface of the cathode that was available for the gliding of rotating gliding discharge channel and decreased the cross-section of the air outlet. The cross-section decrease coupled with the constant air flow leads to the increase of airflow velocity, which caused a faster change of the discharge channel length.

Fig. 4 shows the photograph of the wide-aperture rotating gliding discharge in the quartz reaction chamber at G_d=10 L·min^{-1} air flow and 10 and 50 ms exposure times. Red line shows the orientation of the optical fiber during the measurement of optical emission spectra in the reaction chamber (see Fig. 4). Optical emission spectra were measured alongside the sight line of the optical fiber at the distance h from the lower surface of the quartz reaction chamber (see Fig. 4,b).

Fig. 5 present typical emission spectra of the plasma produced by the wide-aperture rotating gliding discharge in the quartz reaction chamber, which was measured when air without the ethanol (h = 10 mm, I = 60 mA, $G_d = 7{,}5$ L·min^{-1}, G_r=10 L·min^{-1}, Ge = 0 mL·min^{-1}) and with the ethanol flow that corresponded to 5 kW injected into the reaction chamber (h = 10 mm, I = 60 mA, $G_d = 7.5$ L·min^{-1}, $G_r = 10$ L·min^{-1}, Ge = 13.5 mL·min^{-1}) was used as working gas. Spectra are normalized on the average value of intensity between the maximum and the minimum of OH band, which were located at 306.8 and 307.6 nm correspondingly. During the injection of ethanol, spectra (see Fig. 5) show that NO bands and O lines disappear, while the intensity of OH band in the wavelength range of 280…305 nm decrease relative to the intensity of OH band in 305…330 nm range, which can indicate the change of vibrational temperature T_v. The change of the emission spectrum can be connected to the chemical processes that take place during the reforming of ethanol into synthesis gas.

Fig. 6 shows the temperature distribution along the torch inside the reaction chamber for the air flow ($G_d = 7.5$ L·min^{-1}, $G_r = 0$ L·min^{-1}) limited to solely to the discharge chamber (see Fig. 6,a) and air flow ($G_d = 7.5$ L·min^{-1}, $G_r = 10$ L·min^{-1}) inside both discharge and reaction chamber (see Fig. 6,b) determined from the OH band. Electron temperature T_e was determined from the lines of O atoms by using the method of relative intensities. Vibrational T_v and rotational T_r temperatures were determined by comparing the experimental emission spectra with spectra of OH and NO bands modeled by Specair [5]. Results show that obtained temperatures were the same regardless of which bands they were determined from, OH or NO. See Fig. 6 shows that plasma alongside the torch is non-thermal. However, at the ends of the discharge channel, vibrational temperature T_v decreases to the value of rotational temperature T_r. The injection of the additional airflow inside the reaction chamber leads to the decrease of the plasma torch length inside the reaction chamber, which is supported by the data provided on see Fig. 6.

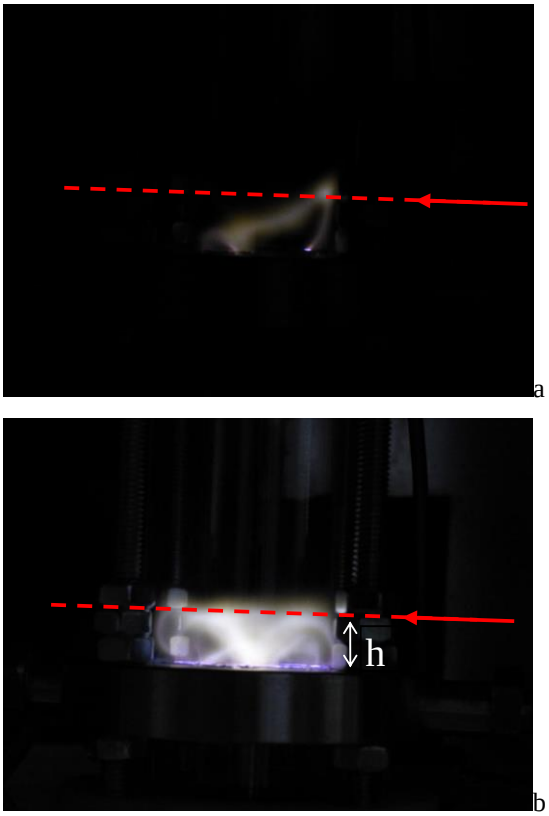

Fig. 4. Photo of rotating gliding discharge at different exposure times: 10 ms (a); 50 ms (b). Red line shows the orientation of optical fiber during optical emission spectra measurement

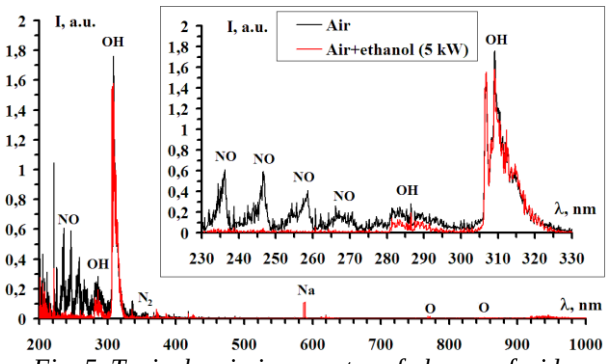

Fig. 5. Typical emission spectra of plasma of wide-aperture rotating gliding discharge in quartz reaction chamber when air without ethanol was used as plasma gas (black) and when ethanol was supplied into system (red) at reaction chamber temperature T_1=200 °C

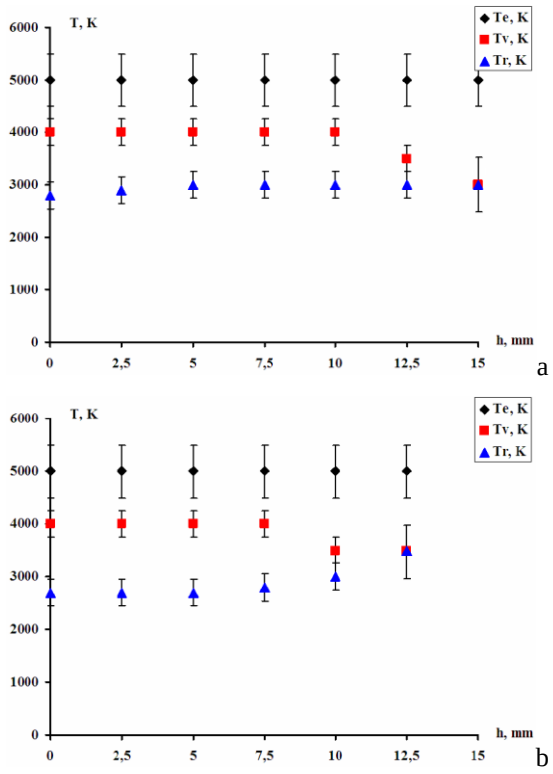

Fig. 6. Temperature distribution along the plasma torch, determined using hydroxyl bands

CONCLUSIONS

The limitation of the surface on which the wide-aperture rotating gliding discharge is able to glide changes the voltage oscillograms by changing the gas dynamics, changing the airflow velocity in this case, which causes faster changes of the discharge channel length. The introduction of the additional airflow into the reaction chamber leads to the decrease of plasma torch inside the reaction chamber. In the case of air flow, the plasma of wide-aperture rotating gliding discharge in the reaction chamber is non-thermal with $T_e>T_v>T_r$. The introduction of ethanol into the reaction chamber causes the disappearance of NO band and O lines from the optical emission spectrum of plasma. This change of emission spectrum can be connected to the chemical processes that occur during the reforming of ethanol into synthesis gas.

ACKNOWLEDGEMENTS

This work was supported in part by the Ministry of Education and Science of Ukraine, National Academy of Sciences of Ukraine, and the Taras Shevchenko National University of Kyiv.

REFERENCES

1. R. Sheldon. Green Chemistry, Catalysis and Valorization of Waste Biomass // *Journal of Molecular Catalysis A: Chemical.* 2016, v. 422, p. 3-12.
2. O.A. Nedybaliuk, V.Ya. Chernyak, I.I. Fedirchyk, et al. Plasma-catalytic reforming of biofuels and diesel fuel // *IEEE Transactions on Plasma Science*. 2017, v. 45. № 7, p. 1803-1811.
3. V. Chernyak, O. Nedybaliuk, O. Tsymbaliuk, et al. Plasma chemistry for concept of sustainable development // *Problems of Atomic Science and Technology*. 2017, № 1, p. 126-131.
4. D.L. Chernolutsky, V.V. Kolgan, V.Ya. Chernyak, et al. Study of the rotating gliding discharge at atmospheric pressure // *Problems of Atomic Science and Technology*. 2014, № 6, p. 175-178.
5. C.O. Laux, T.G. Spence, C.H. Kruger, R.N. Zare. Optical diagnostics of atmospheric pressure air plasma // *Plasma Source Sci. Technol.* 2003, № 2, p. 125-138.
SPECAIR: http://www.specair-radiation.net

Article received 18.10.2018

ПЛАЗМЕННО-КАТАЛИТИЧЕСКОЕ РЕФОРМИРОВАНИЕ ЭТАНОЛА: ВЛИЯНИЕ СТЕПЕНИ АКТИВАЦИИ ВОЗДУХА И ТЕМПЕРАТУРЫ РЕФОРМИРОВАНИЯ

О.А. Недыбалюк, И.И. Федирчик, В.Я. Черняк

Представлены результаты исследования широкоапертурного вращающегося скользящего разряда, который используется для плазменно-каталитического реформирования углеводородов в синтез-газ. Сопоставлены фотографии с осциллограммами напряжения широкоапертурного вращающегося скользящего разряда. Исследованы эмиссионные спектры плазмы факела широкоапертурного вращающегося скользящего разряда в случае подачи только воздуха и подачи смеси воздуха с этанолом в реакционную камеру. Определено распределение температур (электронных T_e, колебательных T_v и вращательных T_r) вдоль плазменного факела в реакционной камере.

ПЛАЗМОВО-КАТАЛІТИЧНЕ РЕФОРМУВАННЯ ЕТАНОЛУ: ВПЛИВ СТУПЕНЮ АКТИВАЦІЇ ПОВІТРЯ ТА ТЕМПЕРАТУРИ РЕФОРМУВАННЯ

О.А. Недибалюк, І.І. Федірчик, В.Я. Черняк

Представлено результати дослідження широкоапертурного обертового ковзного розряду який використовується для плазмово-каталітичного реформування вуглеводнів в синтез-газ. Співставлено фотографії з осцилограмами напруги широкоапертурного обертового ковзного розряду. Досліджено емісійні спектри плазми факелу широкоапертурного обертового ковзного розряду у випадку подачі лише повітря та подачі суміші повітря з етанолом у реакційну камеру. Визначено розподіл температур (електронних T_e, коливних T_v та обертових T_r) вздовж плазмового факела в реакційній камері.